

NAD⁺ Inhibits the Self-Splicing of the Group I Intron

In Kook Park and Jae Young Kim

Department of Biology, Dongguk University, Seoul 100-715, Korea

Received January 3, 2001

We investigated the effects of the coenzyme NAD⁺ (nicotinamide adenine dinucleotide) and its analogs on the self-splicing of primary transcripts of the phage T4 thymidylate synthase gene (*td*). Of all the nicotinamide coenzymes and analogs tested, NADP⁺ was the strongest inhibitor, with a potency approximately threefold that of NAD⁺. Kinetic analysis demonstrated that NAD⁺ acts as a mixed type noncompetitive inhibitor for the *td* intron RNA with a *K_i* of 4.1 mM. The splicing specificity inhibition by NAD⁺ is predominantly due to changes in *K_m* and *k_{cat}*, and was Mg²⁺ concentration dependent. The results suggest that both the ADP and nicotinamide moieties are the key structural features in NAD⁺ responsible for the inhibition of splicing. © 2001 Academic Press

Key Words: T4 phage; group 1 intron; ribozyme; NAD⁺; splicing; noncompetitive inhibition.

The T4 phage thymidylate synthase gene (*td*) undergoes the self-splicing *in vitro* in the absence of any protein factors or energy source (1). Like the intron in the nuclear large rRNA gene of *Tetrahymena thermophila* (2), the *td* intron is processed from a precursor RNA via a series of the transesterification mechanism (3).

The self-splicing reaction of group I introns has been shown to be inhibited by a number of small molecules. The guanosine analogs deoxyguanosine and dideoxyguanosine (4), the amino acid arginine (5) and the antibiotics streptomycin (6), viomycin and di-β-lysylcapreomycin (7) are competitive inhibitors of the self-splicing via their guanidino groups, which they have in common with the cofactor guanosine. However, the pseudosaccharide lysinomycin (8) which does not contain a guanidino group also inhibits the self-splicing by a competitive interaction. Recently we found that the coenzyme FMN acts as a competitive inhibitor for the *td* intron RNA with a *K_i* of 1.86 mM although it does not possess a guanidino group in its structure (9).

However, aminoglycoside antibiotics of neomycin, gentamicin, kanamycin and tobramycin (10), tetracycline

and pentamidine (11), and spectinomycin (12) which do not have guanidino groups are noncompetitive inhibitors of the group 1 intron splicing. In contrast, some simple molecules, such as monovalent cations (13, 14), polyamines (15) and antibiotic tuberactinomycin enhance the RNA function (16).

NAD⁺ is a major coenzyme of dehydrogenases that mediate various cellular oxidation-reduction reactions (17). During this reaction, NAD⁺ accepts a hydride ion from the substrate molecule undergoing the oxidation. NAD⁺ has been also considered as a remnant of the transition from the earlier “RNA world” since it has RNA components in its structure (18). Recently, the recognition of RNA by NAD⁺ has been demonstrated using the *in vitro* selection of RNA that bind this coenzyme (19–21).

Due to its biological importance as a major coenzyme in the cellular metabolism and its structural resemblance to ribonucleotides we attempted to examine whether NAD⁺ and its analogs (Fig. 1) inhibit the self-splicing of primary transcripts of the phage T4 thymidylate synthase gene *in vitro* and to determine the key structural features of NAD⁺ responsible for splicing inhibition.

MATERIALS AND METHODS

Bacterial strains and plasmids. *Escherichia coli* strains TG1 and HB101 were obtained from Amersham. M13mp8 phage was purchased from Bethesda Research Laboratories and pGEM-2 vectors were from Promega Corp.

Enzymes and chemicals. NAD⁺ and its analogs were obtained from Sigma Chemical Co. Restriction enzymes *EcoRI* and *HindIII* were obtained from New England Biolabs. [α -³²P]GTP (>400 Ci/mmol) was obtained from Amersham. Nucleoside triphosphates were obtained from Boehringer Mannheim. T7 RNA polymerase (20 U/μl) was obtained from United States Biochemical and RNasin (40 U/μl) and RQ1 DNase (1 U/μl) from Promega Corp.

Construction and preparation of recombinant plasmids. The cloning procedures were as described previously (1). The pGEM recombinant containing 390 nt of the 5' exon 1, 1016 nt of the intron and 824 nt of the 3' exon 2 were kindly provided by Dr. Fred Chu. The pGEM recombinant plasmids were transformed into *E. coli* HB101 cells, propagated in the presence of ampicillin and amplified in the presence of chloramphenicol (22). The promoter alignment of the *td* fragment was determined by 0.8% agarose gel analysis of restriction fragments from pGEM-2 recombinant plasmids.

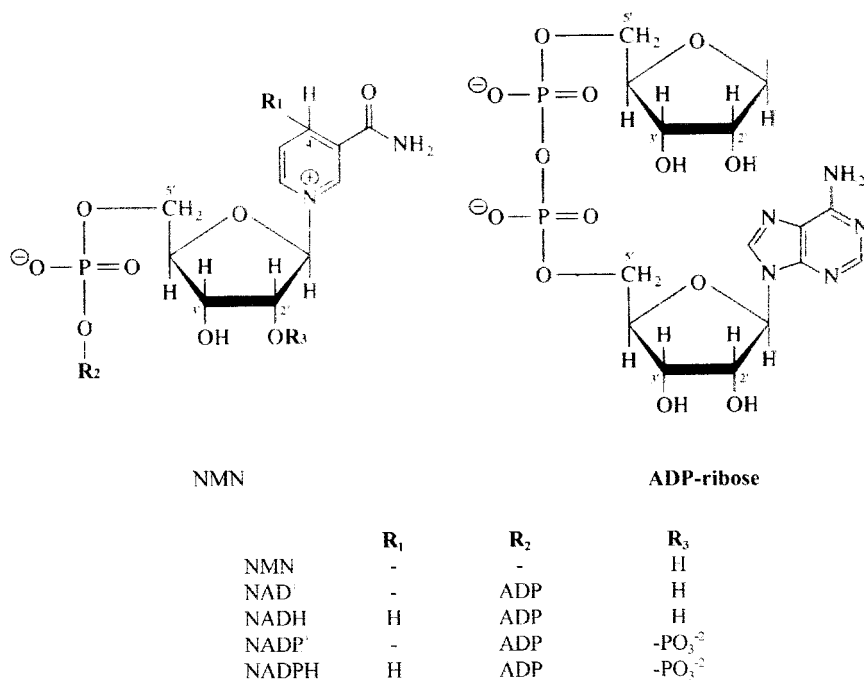


FIG. 1. The chemical structures of NAD⁺ and its analogs.

Synthesis of RNA by *in vitro* transcription. The pGEM recombinant plasmids were linearized with *Hpa*I which cuts the *td* fragment once at 520 bp downstream of exon 2. Each linearized recombinant plasmid DNA was used as a template for *in vitro* transcription following deproteinization by phenol extraction and ethanol precipitation. The transcription was performed at 30°C for 40 min in the transcription buffer (40 mM Tris-HCl, pH 7.5, 3 mM MgCl₂, 1 mM spermidine, 5 mM NaCl), 10 mM DTT, 1 U/ml RNasin, 0.5 mM of each rNTP, 5 μ Ci of [α -³²P] GTP, and 10 U of T7 RNA polymerase. The RNA synthesis was terminated by the addition of RQ1 DNase to destroy the DNA template. Following the transcription, the synthesized 2.23 kb primary transcript was purified free of proteins, ribonucleotides and salts by passage through a Nensorb²⁰ cartridge (DuPont). The bound RNA was eluted with 20% ethanol from the cartridge, followed by precipitation with 2 volumes of ethanol in the presence of 0.2 M sodium acetate. The RNA precipitate was washed three times with 70% ethanol to remove salts.

***In vitro* self-splicing reaction.** The splicing reaction buffer contained 40 mM Tris-HCl, pH 7.4, 5 mM MgCl₂, 100 μ M GTP and 8 nM RNA. Varying concentrations of NAD⁺ and its analogs were added to the reaction buffer to examine their effects on the splicing. At the end of incubation, the reaction mixture was centrifuged briefly to collect the moisture, chilled on ice and 5 μ l of the sample buffer (95% deionized formamide, 10 mM Na₂EDTA, 0.08% xylene cyanol, 0.08% bromophenol blue) was added. The spliced RNA products were electrophoresed in a 0.75 mm thick slab gel containing 4% polyacrylamide and 8 M urea in TBE buffer (0.1 M Trizma base, 0.1 M boric acid, 2 mM Na₂EDTA) and visualized by autoradiography without drying. Autoradiograms were scanned and integrated with a Hoefer image analyzer.

Kinetic analysis. For the kinetic analysis the splicing reaction was performed by incubating precursor RNAs of the *td* intron RNA in the presence of varying concentrations of GTP (0.5, 1, 2, 5, 20 and 100 μ M) and in the absence or presence of 4 and 5 mM NAD⁺ for 2 up to 6 min. The accumulated splicing products were determined from the densitometric analysis with Hoefer image analyzer. The ratio of the E1-E2 ligation product to the total spliced products (I-E2 + I-E1 +

E1-E2 + CI + LI) plus the remaining pre-RNAs was calculated and the initial velocities were calculated from the percentage of the E1-E2 ligation product formed per min. The reciprocal of the initial velocity was plotted against the reciprocal of GTP concentration in the absence or presence of 4 or 5 mM NAD⁺. The *K_i* value for NAD⁺ was determined by plotting 1/*V* versus varying concentrations of NAD⁺ in the presence of different fixed concentrations of GTP as indicated in the figure legend.

RNA concentration. The RNA concentration was determined by the spectrophotometric method (23). The extinction coefficient was determined by hydrolyzing the RNA to nucleotides and by measuring the *A*₂₆₀ value of the resulting mixture.

RESULTS

Inhibition of the td Intron RNA Splicing by NAD⁺

As shown in Fig. 2A, the progressive inhibition by NAD⁺ is evident from the decreases in splicing products when NAD⁺ concentration increases (Fig. 2A). At 5 mM the splicing activity was inhibited about 30% that of the normal splicing activity (Fig. 2B). When the NAD⁺ concentration was increased, the formation of I-E2 intermediate, E1-E2 ligation product, linear and circular introns was decreased accordingly and at 10 mM the splicing was almost abolished.

NAD⁺ and Its Analogs as Splicing Inhibitors

We screened a range of structurally related members of NAD⁺ in splicing inhibition assays to establish the relationships between the structure of NAD⁺ and splicing activity of intron RNA. The inhibitory concentrations of NAD⁺ and its analogs required to cause 50%

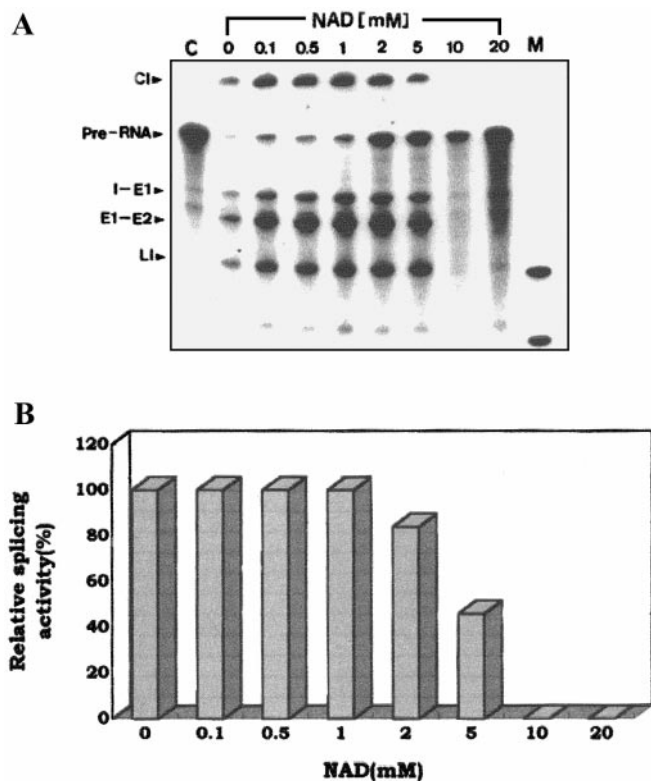


FIG. 2. Inhibition of the self-splicing of the phage T4 *td* intron RNA by NAD^+ . (A) Autoradiograms showing the splicing activity in the presence of varying concentrations (0–20 mM) of NAD. Lane 1, unspliced pre-RNA; I-E2, intron–exon 2; LI, linear intron; CI, circular intron; E1-E2, exon 1–exon 2 ligation product. (B) Splicing rates of the *td* intron RNA as a function of concentrations of NAD^+ . The relative inhibition was expressed as the percentage reduction in the formation of E1-E2 ligation product in the presence of NAD^+ with respect to that observed in the absence of NAD^+ .

inhibition for the splicing activity are presented in Table 1. The comparison of analogs shows the order of the inhibitory efficiency for the self-splicing as follows: $\text{NADP}^+ > \text{NAD}$, NADH , $\text{NADPH} > \text{ADP-ribose} > \text{NMN}$

TABLE 1

NAD^+ and Its Analogs as Inhibitors of the Self-Splicing of the *td* Intron RNA

Compounds	Inhibitory concentration
NAD^+	5 mM
NADH	5 mM
NADP^+	4 mM
NADPH	5 mM
NMN	n.i. (up to 20 mM)
ADP-ribose	10 mM

Note. The precursor RNA of the phage T4 *td* intron was incubated under splicing conditions with varying concentrations of NAD^+ and its analogs. The values indicate the concentration of compounds needed to cause 50% inhibition of the splicing. n.i., no inhibition.

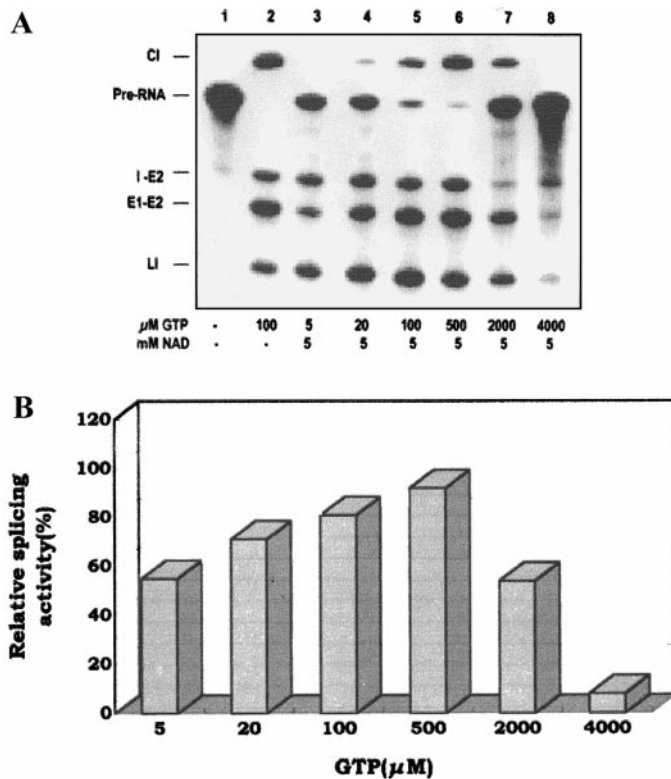


FIG. 3. Effect of GTP on the splicing inhibition by NAD^+ . (A) Autoradiograms showing the splicing activity in the presence of varying concentrations of GTP at the fixed concentration of 5 mM NAD. Lane 1, unspliced pre-RNA; lane 2, normal splicing; lane 3, 5 μM GTP; lane 4, 20 μM GTP; lane 5, 100 μM GTP; lane 6, 500 μM GTP; lane 7, 2000 μM GTP; lane 8, 4000 μM GTP. I-E2, intron–exon 2; LI, linear intron; CI, circular intron; E1-E2, exon 1–exon 2 ligation product. (B) Relative splicing activities of the *td* intron RNA as a function of concentrations of GTP. The relative splicing rate was expressed as the percentage of the formation of E1-E2 ligation product of each reaction to that of the normal splicing reaction.

(nicotinamide mononucleotide). Of all compounds tested, NADP was the most potent, showing 50% inhibition at 4 mM and NAD, NADH, and NADPH were the next strong inhibitors (5 mM). ADP-ribose was relatively weak inhibitors (10 mM) compared to NADP and NAD. NMN virtually had no effects on the splicing activity.

Effect of GTP on the Splicing Inhibition by NAD^+

As shown in Fig. 3, the splicing activity increased gradually as the concentration of GTP increased up to 500 μM . Above 500 μM GTP, however, the splicing activity decreased markedly. The splicing inhibition by NAD^+ was not reversed at a high concentration of GTP, thereby suggesting a noncompetitive nature of inhibition.

Effect of Mg^{2+} on the Splicing Inhibition by NAD^+

Effect of Mg^{2+} on the splicing inhibition by NAD^+ is shown in Fig. 4. At 3 mM Mg^{2+} the splicing rate de-

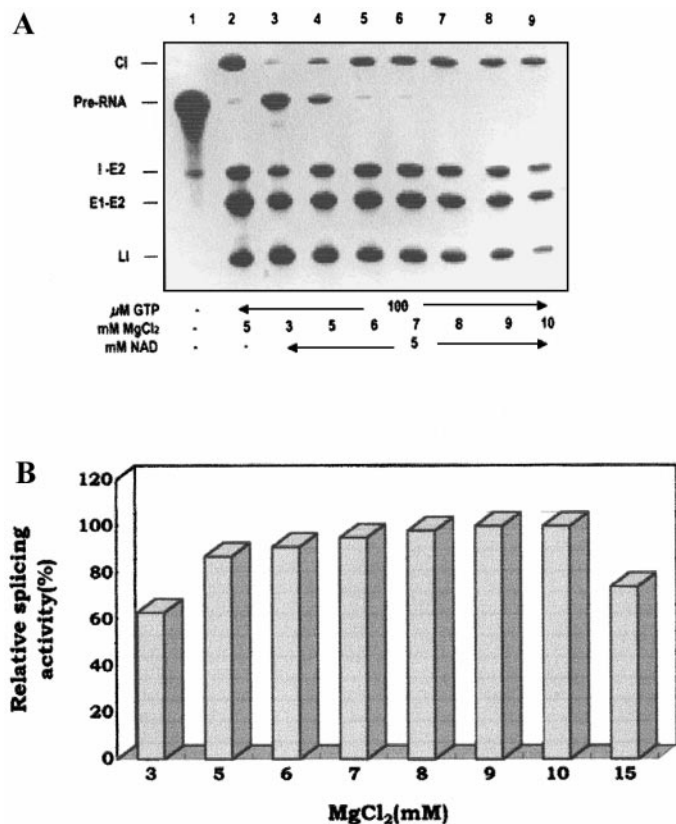


FIG. 4. Effect of Mg^{2+} on the splicing inhibition by NAD^+ . (A) Autoradiograms showing the splicing activity in the presence of varying concentrations (3–10 mM) of Mg^{2+} . Lane 1, unspliced pre-RNA; lane 2, normal splicing; lane 3, 3 mM Mg^{2+} + 5 mM NAD^+ ; lane 4, 5 mM Mg^{2+} + 5 mM NAD^+ ; lane 5, 6 mM Mg^{2+} + 5 mM NAD^+ ; lane 6, 7 mM Mg^{2+} + 5 mM NAD^+ ; lane 7, 8 mM Mg^{2+} + 5 mM NAD^+ ; lane 8, 9 mM Mg^{2+} + 5 mM NAD^+ ; lane 9, 10 mM Mg^{2+} + 5 mM NAD^+ . I-E2, intron-exon 2; LI, linear intron; CI, circular intron; E1-E2, exon 1-exon 2 ligation product. (B) Relative splicing activities of the *td* intron RNA as a function of concentrations of Mg^{2+} . The ratio of E1-E2 ligation produced in each splicing reaction to that of the normal splicing reaction was expressed as the relative splicing activity.

creased by about 38% relative to that of the normal splicing. Increasing the Mg^{2+} concentration restored the splicing activity inhibited by NAD^+ up to 10 mM concentration above which the splicing activity dropped to about 30% (Fig. 4B). At 10 mM Mg^{2+} the splicing rate was restored back to close to that of the normal splicing activity. However, at a higher concentration than 10 mM Mg^{2+} the splicing rate was reduced by about 27%. Thus overall results demonstrate that the inhibition by NAD^+ was Mg^{2+} dependent, presumably interfering with the catalytic function of Mg^{2+} in the self-splicing reaction.

Kinetic Studies

To test whether the inhibition by NAD^+ was competitive or noncompetitive with GTP, varying concentra-

tions of NAD^+ were incubated with varying concentrations of GTP for 2 to 6 min (Fig. 5A). As the concentration of GTP increased up to 100 μ M in the presence of 4 mM NAD^+ , the splicing rate was substantially recovered, reaching almost 80% that of the normal splicing rate. However, at 5 mM NAD^+ the restoring effect by GTP was very minimal. Even 500 μ M GTP did not alleviate the splicing inhibition by NAD^+ (data not shown). This suggests that NAD^+ inhibition of the self-splicing reaction was not reversed at a high con-

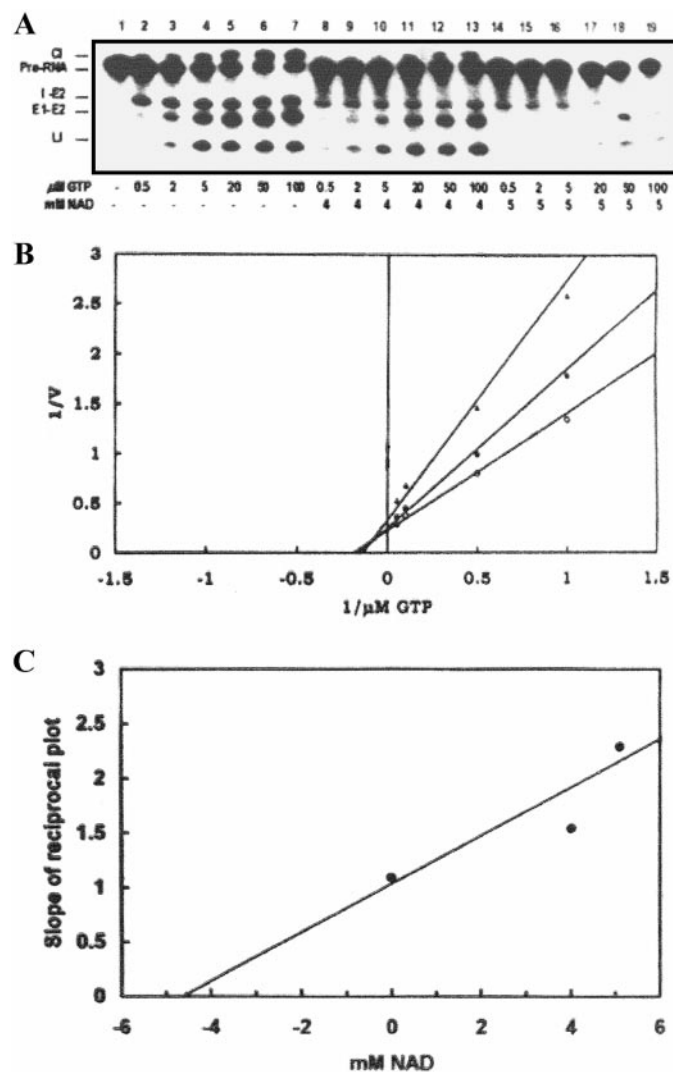


FIG. 5. Mixed noncompetitive inhibition of the T4 *td* intron RNA splicing by NAD^+ . (A) Autoradiogram of splicing products in the absence or presence of NAD^+ . (B) Lineweaver-Burk plot showing the noncompetitive inhibition of splicing of the *td* intron RNA by NAD^+ . The band densities on gels were quantitated on a densitometer and the initial velocity was calculated from the percentage of spliced products formed per minute. The reciprocal initial velocities of the formation of splicing products are plotted versus $1/[GTP]$ for different concentrations of NAD^+ . \circ , 0 mM NAD^+ ; \bullet , 4 mM NAD^+ ; \blacktriangle , 5 mM NAD^+ . (C) Determination of the K_i value of NAD^+ inhibition. The K_i for NAD^+ was determined by plotting the slopes of the Lineweaver-Burk plot versus the concentration of NAD^+ .

TABLE 2
Kinetic Parameters of the Self-Splicing
of the Phage T4 *td* Intron RNA

	K_m (μM)	V_{\max} (nM/min)	k_{cat} (min^{-1})	k_{cat}/K_m ($\text{M}^{-1} \text{min}^{-1}$)
No NAD^+	5.2 ± 0.4	0.38 ± 0.03	0.048 ± 0.004	9.2×10^3
4 mM NAD^+	6.1 ± 0.5	0.33 ± 0.03	0.041 ± 0.003	6.7×10^3
5 mM NAD^+	7.3 ± 0.7	0.25 ± 0.03	0.031 ± 0.004	4.2×10^3

Note. Values are the means \pm SE of 3 experiments. K_m and k_{cat} values were determined directly by fitting the Lineweaver-Burk plot at varying concentrations of GTP concentrations (0.5, 2, 5, 20, 50, 100 μM). The concentration of the precursor RNAs used for the splicing reaction was 8 nM.

centration of GTP, indicating a noncompetitive nature of the inhibition.

The fact that all lines intersect to the left of the $1/v$ axis indicates that NAD^+ is a mixed noncompetitive inhibitor for the self-splicing with GTP (Fig. 5B). The slopes and intercepts reveal that NAD^+ does not compete with GTP for binding to the intron RNA. The calculated K_i value for the NAD^+ inhibition of the self-splicing was 4.1 mM (Fig. 5C). The kinetic parameters for the self-splicing of the *td* intron RNA are presented in Table 2. The K_m values for GTP in the presence of 4 mM and 5 mM NAD^+ are 6.1 μM and 7.3 μM , respectively, indicating the interference of NAD^+ with the affinity of GTP for the intron RNA. As expected, V_{\max} values are lowered by 0.86-fold and 0.65-fold, respectively. Increasing the NAD^+ concentration raised the K_m values with corresponding decreases of V_{\max} and k_{cat} values. The increase in K_m and the decrease in k_{cat} resulted in a decrease of the k_{cat}/K_m values. The results suggest that the specificity of the splicing inhibition by NAD^+ is manifested primarily as changes in both K_m and k_{cat} .

DISCUSSION

The coenzyme NAD^+ inhibited the first step of the transesterification for the self-splicing of the *td* intron RNA in a noncompetitive manner. The first step inhibition was mostly observed with molecules with guanidino residues such as streptomycin (6), arginine (5), guanosine analogs (4), and tuberactinomycin peptides (7) which was due to the competition with the binding of the guanosine cofactor for the G-binding site located in the core of the intron RNA (24). Even if NAD^+ does not possess a guanidino group in the structure, it interfered with the first step of the self-splicing as a mixed type noncompetitive inhibitor for the *td* intron RNA. A similar observation was also made with the coenzyme FMN which does not possess a guanidino residue and interferes with the first step of the self-splicing of the *td* intron RNA as a competitive inhibitor

(9). Like FMN, NAD^+ demonstrates the structural specificity in inhibiting the splicing for the *td* intron RNA.

The comparison of the K_i values of other known competitive inhibitors for the group I intron RNA demonstrated that NAD^+ (4.1 mM) is stronger than most competitive inhibitors such as streptomycin (5 mM), arginine (8.3 mM), and dideoxy GTP (5.3 mM) but weaker than FMN (1.86 mM), viomycin (17 μM) and di- β -lysylcapreomycin IIA (8.5 μM) (6, 5, 4, 9, 7). The kinetic parameters that are influenced significantly by NAD^+ is the K_m and k_{cat} values. The K_m of the intron RNA for GTP is about 1.4-fold higher at 5 mM NAD^+ than in its absence, suggesting a slight alteration in the affinity of the intron RNA for GTP.

The inhibitory action of NAD^+ at 5 mM concentration on the splicing activity was also found to be dependent on the Mg^{2+} concentration whereas that of NADP^+ was not (data not shown). If the interaction of NAD^+ with the intron RNA is ionic, increasing concentrations of Mg^{2+} should alleviate the NAD^+ inhibition of the splicing activity by acting as a competing counterion. This appears to be what happened in the present study. One possibility is that Mg^{2+} ions may neutralize the overall charges of NAD^+ , thus possibly protecting the splicing activity from the inhibition by NAD^+ . Besides its role as a catalytic cofactor, Mg^{2+} is thought to be involved in the proper folding and general electrostatic interactions to shield the phosphodiester backbone (25, 26). Similarly, the splicing inhibition by FMN (9) was partially reversed by enhancing Mg^{2+} concentration whereas that by viomycin and tuberactinomycin was fully reversed (7).

The results show that the inhibitory effect of NAD^+ is dependent on not only the GTP concentration but also the Mg^{2+} concentration. This implies that NAD^+ may possibly interact with other specific sites within the intron RNA structure which could be Mg^{2+} -binding sites although its inhibitory mechanism is not fully understood yet. Recently the antibiotic neomycin B has been shown to inhibit the self-splicing of the *td* intron RNA by binding to the internal loop between the stems P4 and P5 and displacing Mg ions in the catalytic core (27). Another possibility is that in the interaction of NAD^+ -RNA complex the hydrogen bonds and base-stacking interactions could play a significant part of contributions in inhibiting RNA splicing (28).

Of all analogs tested, NADP^+ was the most inhibitory and its potency was approximately three-fold higher than that of NAD^+ which mainly differ from NADP^+ in lacking one phosphate group. Interestingly enough, the presence of one additional phosphate group of NADP^+ somehow stimulated its inhibitory potency. Although its mechanistic role is not clear yet, there is a possibility that one additional phosphate group may interfere with either the binding or the catalytic action of Mg^{2+} ion. Similar observations have

been also made with aminoglycoside antibiotics in which a single substitution of a hydroxy group in paromomycin with an amino group produces neomycin B (29). In fact, neomycin B inhibits the self-splicing of the *td* intron RNA at 100-fold lower concentration than that of paromomycin. In general, amino groups favor the splicing inhibition due to the interaction of protonated amino groups of these antibiotics with the negative charges of the intron RNA backbone. Thus it can be suggested that similar situations may occur with NAD⁺ despite its structural discrepancy.

On the basis of the inhibitory concentration and structural examination of NAD⁺ and its analogs we assume that a key structural feature in NAD⁺ responsible for the inhibition of self-splicing reaction may be both ADP and nicotinamide. In addition, it was of interest that the coenzyme NAD⁺ inhibited the first step of self-splicing of the *td* intron RNA as a noncompetitive inhibitor although it does not have a guanidino group. The finding of NAD⁺ as a potent inhibitor specific for the self-splicing of the group I intron RNA reveals another new class of inhibitors. This unique role of NAD⁺ in splicing reaction of the *td* intron RNA prompted us to propose that this coenzyme could have played a very prominent role in the gene regulation in RNA world as well as in the contemporary cellular metabolism (18). The examination of the NAD⁺-intron RNA complex by the footprinting or the NMR experiments could help to identify the specific functional groups involved in the interaction of NAD⁺ with the intron RNA. Due to its biological importance as an electron carrier in the redox reaction and structural simplicity, the coenzyme NAD⁺ can be employed for developing the potential pharmaceutical agents against RNA pathogens.

ACKNOWLEDGMENTS

We thank Dr. Fred K. Chu for his generous gift of the pGEM recombinant plasmids. This work was supported by a grant of Genetic Engineering Research Program (1997–1998) from the Ministry of Education of the Republic of Korea.

REFERENCES

1. Chu, F. K., Maley, G. F., Maley, F., and Belfort, M. (1994) *Proc. Natl. Acad. Sci. USA* **81**, 3049–3053.
2. Cech, T. R., Tanner, N. K., Tinoco, I., Jr., Weir, B. R., Zuker, M., and Perlman, P. S. (1983) *Proc. Natl. Acad. Sci. USA* **80**, 3903–3907.
3. Chu, F. K., Maley, G. F., West, D. K., Belfort, M., and Maley, F. (1986) *Cell* **45**, 157–166.
4. Bass, B., and Cech, T. R. (1986) *Biochemistry* **25**, 4473–4477.
5. Yarus, M. (1988) *Science* **240**, 1751–1758.
6. von Ahsen, U., and Schroeder, R. (1991) *Nucleic Acids Res.* **19**, 2261–2265.
7. Wank, H., Rogers, J., Davies, J., and Schroeder, R. (1994) *J. Mol. Biol.* **236**, 1001–1010.
8. Rogers, J., and Davies, J. (1994) *Nucleic Acids Res.* **24**, 4983–4988.
9. Kim, J. Y., and Park, I. K. (2000) *Biochim. Biophys. Acta* **1475**, 56–61.
10. von Ahsen, U., Davies, J., and Schroeder, R. (1991) *Nature* **353**, 368–370.
11. Liu, Y., Tidwell, R. R., and Leibowitz, M. J. (1994) *J. Euk. Microbiol.* **41**, 31–38.
12. Park, I. K., Lim, E. H., and Park, I. K. (2000) *Biochem. Biophys. Res. Commun.* **269**, 574–579.
13. Collins, R. A., and Olive, J. E. (1993) *Biochemistry* **32**, 2795–2799.
14. Park, I. K., and Sung, J. S. (2000) *Biochim. Biophys. Acta* **1492**, 94–99.
15. Dahm, S. A., and Uhlenbeck, O. C. (1991) *Biochemistry* **30**, 9464–9469.
16. Olive, J. E., De Abreu, D. M., Rastogi, T., Andersen, A. A., Mittermaier, A. K., Beattie, T. L., and Collins, R. A. (1995) *EMBO J.* **14**, 3247–3251.
17. Buggs, T. (1997) *An Introduction to Enzyme and Coenzyme Chemistry*, Blackwell Science.
18. White, H. B. (1976) *J. Mol. Biol.* **7**, 101–104.
19. Burgstaller, P., and Famulok, M. (1994) *Angew. Chem.* **33**, 1084–1087.
20. Lauhon, C. T., and Szostak, J. W. (1995) *J. Am. Chem. Soc.* **117**, 1246–1257.
21. Fan, P., Suri, A. K., Fiala, R., Live, D., and Patel, D. J. (1996) *J. Mol. Biol.* **258**, 480–500.
22. Shin, S., and Park, I. K. (1993) *J. Biochem. Mol. Biol. (formerly Korean Biochemical J.)* **26**, 614–619.
23. Puglisi, J. D., and Tinoco, I., Jr. (1989) *Methods Enzymol.* **180**, 304–325.
24. von Ahsen, U., and Schroeder, R. (1990) *Nature* **346**, 801.
25. Grosshans, C. A., and Cech, T. R. (1989) *Biochemistry* **28**, 6888–6894.
26. Celander, D. W., and Cech, T. R. (1991) *Science* **251**, 401–407.
27. Hoch, I., Berens, C., Westhof, E., and Schroeder, R. (1998) *J. Mol. Biol.* **282**, 557–569.
28. Burgstaller, P., Hermann, T., Huber, C., Westhof, E., and Famulok, M. (1997) *Nucleic Acids Res.* **25**, 4018–4027.
29. Von Ahsen, U., Davies, J., and Schroeder, R. (1992) *J. Mol. Biol.* **226**, 935–941.